

# An Atmospheric Attenuation Model for a Proposed K-band Near-Earth Uplink Frequency Band

David D. Morabito\*

**ABSTRACT.** — A new uplink frequency band (22.55–23.15 GHz) is being planned for use in lunar communications. Since this frequency band lies next to the peak of the water vapor absorption line, atmospheric attenuation statistics were derived from sky brightness temperatures at the lower frequency channels of water vapor radiometers (WVRs) used in the DSN. This article details the approach used to generate these statistics for the three DSN tracking complexes, and presents the statistics for availabilities of 90% and 95%, planned for use in lunar link budgets. Best-month and worst-month statistics are also provided, which can serve as favorable or conservative entries for atmospheric attenuation in telecom link budget tables, respectively.

## I. Introduction and Requirements

An atmospheric model is needed for the proposed near-Earth communications band for uplink high-rate lunar communications. The Interagency Operations Advisory Group (IOAG) recommendations for lunar communication allocate 22.55–23.15 GHz (600 MHz bandwidth) for K-band uplink [1]. The average center frequency of the band is 22.85 GHz. Atmospheric models currently exist for the deep-space network (DSN) tracking sites of Goldstone, Canberra, and Madrid at the 32 GHz (Ka-band), 26 GHz (K-band), 8.4 GHz (X-band) and 2.3 GHz (S-band) downlink frequency bands [2]. These models were generated from multiple years of water vapor radiometer (WVR) sky brightness temperature<sup>1</sup> (TB) data at 31.4 GHz [2]. The Ka-band (32 GHz) estimates of atmospheric noise temperature and atmospheric attenuation statistics were derived directly from the 31.4 GHz channel WVR TB by applying adjustments for cosmic background and frequency-difference. A similar method was used for S-band, X-band, and K-band [2].

The proposed 22.85 GHz frequency band cumulative distributions (CDs) for atmospheric attenuation were derived from WVR TB measurements at nearby frequencies adjacent to

---

<sup>1</sup> Sky brightness temperature is defined as  $TB = T_{atm} + T_c/L_{atm}$  where  $T_{atm}$  is the atmosphere noise temperature,  $T_c = 2.725$  K is the cosmic background and  $L_{atm} = 10^{(A/10)}$  where  $A$  is the atmospheric attenuation in dB.

---

\* Communications Architectures and Research Section.

the band and from International Communication Union (ITU) models ([3] references therein). The TB at the WVR channel frequencies and selected frequencies over the 22.55–23.15 GHz band were independently estimated using ITU models of atmospheric noise temperature [3] along with adjustments for the cosmic background. The ITU model values of TB at the WVR channel frequencies were appropriately scaled to match the measured values of TB from the WVRs. The derived scaling coefficients were then applied to the ITU model values within the 22.55–23.15 GHz band. The TB were converted to atmospheric noise temperatures, which were then converted to atmospheric attenuation using equations and methods outlined in the DSN Telecommunications Link Design Document [2] (referred to as the 810-005 document). All data, statistics, and curves presented in this article are referred to zenith. A process to adjust the statistics to different elevations can be performed using the formulation provided in [2].

## II. Analysis Approach

The 22.85 GHz frequency band lies very close to the water vapor absorption line at 22.235 GHz. The advanced WVR (AWVR) used for Goldstone and Madrid has three frequency channels centered at 22.2, 23.8, and 31.4 GHz, each with 400 MHz bandwidths. Since the 22.2 and 23.8 channels lie close to the water vapor absorption line, one can use the AWVR data at these frequencies to derive the statistics for the 22.55–23.15 GHz band. This was accomplished in a similar manner as was done in previous years by using the 31.4 GHz channel TB measurements to generate the 32 GHz atmospheric attenuation and atmospheric noise temperature statistics for the DSN [2]. Since no WVR channels lie inside the 22.55–23.15 GHz band, the ITU model estimates at these frequencies can provide curve shape information for the adjustments. Thus, the 22.2 and 23.8 GHz AWVR derived temperatures serve as “pivot” points to appropriately scale the ITU values. An earlier study documents the comparison between the 810-005 model (based on WVR measurements) and the ITU model [3].

Since the AWVR channels lie near the peak of the water vapor absorption line, it was deemed instructive to first perform a comparison of measured sky brightness from the AWVR against that derived from ITU models for all three channels. Thus, one could infer the utility of using the ITU model at 22.85 GHz from these results. Figure 1 displays the total attenuation and vapor attenuation as a function of frequency for Goldstone assuming zenith (90 deg elevation) and 90% availability based on ITU models. These curves follow the general shape of the water vapor absorption line attributed to Liebe [4]–[5] but applicable to the Goldstone climate. The span of the three Goldstone/Madrid AWVR channels are shown by the flat bars at 0.75 dB, those of the Canberra WVR channels at 0.6 dB, and the span of the 22.55–23.15 GHz frequency band denoted by the flat bar at 0.9 dB. The two AWVR channels centered at 22.2 GHz and 23.8 GHz lie on either side of the 22.85 GHz band, and are beneficial for use to generate attenuation statistics for this band. The AWVR/WVR points can serve as anchors to match the ITU model values, and thus allows the ITU curve to be adjusted up or down to yield attenuation values within the proposed band at selected frequencies of 22.55, 22.65, 22.75, 22.85, 22.95, 23.05, and 23.15 GHz.

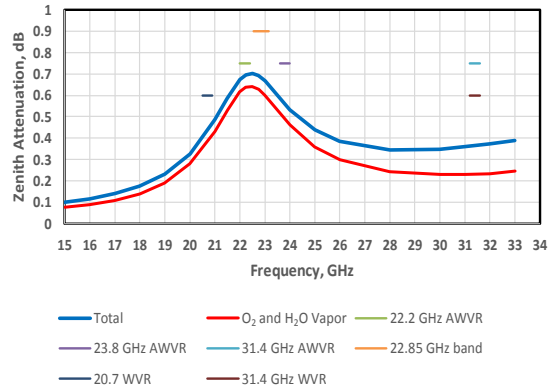


**Figure 1. Total attenuation (including liquid water) (blue) and water vapor and oxygen attenuation (red) vs. frequency for Goldstone at zenith and 90% availability based on ITU models. Also shown are the spans of the Goldstone and Madrid AWVR channels (0.75 dB), Canberra WVR channels (0.6 dB), and proposed uplink 22.55–23.15 GHz band (0.9 dB).**

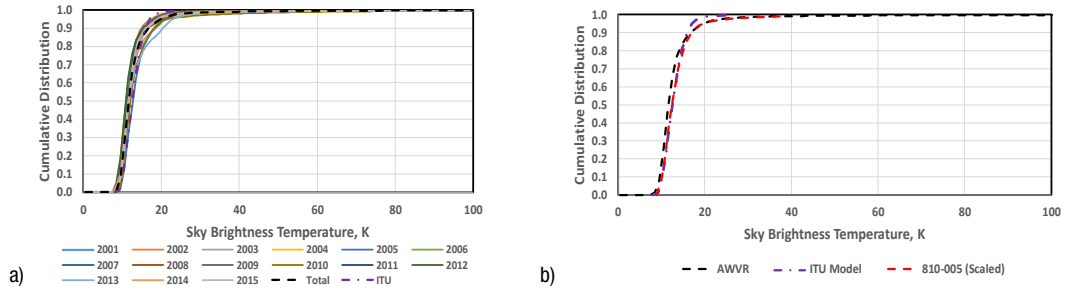
Since data from an older WVR model was used for Canberra, only two frequency channels were available, one at 20.7 GHz and one at 31.4 GHz. Thus, for Canberra, the 20.7 GHz channel results were used to anchor the ITU curve values at this frequency. The derived offset was then used to scale the ITU curve values across the 22.55 to 23.15 GHz band frequencies.

### III. Analysis Results

#### A. Goldstone, California

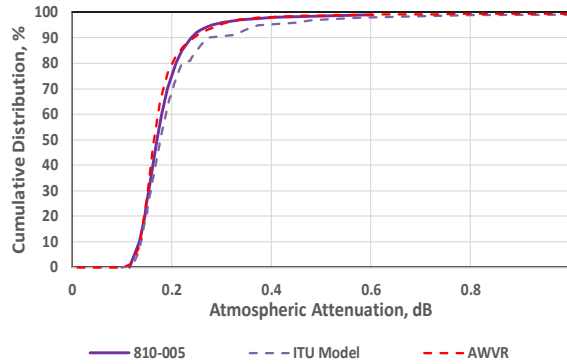
Fifteen years of AWVR data from Goldstone spanning the period from 2001 to 2015 were used for this analysis. Figure 2a displays the cumulative distribution (CD) curves for the 31.4 GHz channel TB. Here the individual year AWVR CDs are represented by solid colors, the mean CD of the AWVR data by the black dashed curve, and the CD of the TB derived from the ITU model by the dashed purple curve.

Figure 2b displays the mean TB CD curve derived from the AWVR 31.4 GHz channel data (dashed black), the TB CD curve derived from the ITU model at 31.4 GHz (dashed purple), and the TB curve derived from the 810-005 document 32 GHz atmospheric noise temperature data adjusted to 31.4 GHz (dashed red). Here, the AWVR curve is consistent with that derived from the DSN 810-005 document statistics as expected (after adjusting for cosmic background and frequency difference) [2]. The agreement is not exact as the 810-005 document curves were derived from data spanning a wider range of time including the use of data from other WVR models. The agreement shown here provides



**Figure 2. a) CD of TB at 31.4 GHz: AWVR mean (dashed black), AWVR individual years (solid colors) and ITU model (dashed purple). b) CD of TB at 31.4 GHz: mean AWVR from Figure 1 (black dashed), ITU model (purple dashed), and 810-005 document atmospheric noise temperature adjusted to 31.4 GHz.**

confidence in the AWVR data set used in this study as well as providing a consistency check with statistics derived years earlier with similar WVR data over different time spans. Here, the ITU model curve shows higher values at low CDs with the difference running  $\sim 1$  K. At higher CDs above 90%, the differences become somewhat larger. The ITU model originally showed much higher values at the higher CDs, but the 0.01% rain rate input to the ITU rain model was deemed excessive, so a more reasonable rain rate was used [3], resulting in closer agreement. Figure 3 displays the corresponding CD values for zenith atmospheric attenuation at 32 GHz where we see very good agreement between the AWVR derived values from 2001–2015 (dashed red), with the 810-005 tabulated values (solid purple). Here, the ITU derived values start to deviate at the higher CDs likely due to deficiencies in the ITU rain/cloud models or their inputs.



**Figure 3. Cumulative distribution of zenith atmospheric attenuation at 32 GHz; AWVR adjusted (red dashed), ITU model (purple dashed) and 810-005 document [2] atmospheric attenuation (solid purple).**

Since the AWVR frequency channels at 22.2 and 23.8 GHz lie adjacent to the 22.55–23.15 GHz band, it was deemed appropriate to generate the CDs from these data, with the ITU model providing curve shape information for adjustment. The AWVR 22.2 and 23.8 GHz channel data were processed in the same manner as was done for the 31.4 GHz channel. The ITU model curves were also generated at these frequencies.

Figure 4a displays the CD curves for the 22.2 GHz channel for the individual years (solid colors) as well as the AWVR mean (dashed black) and ITU model (dashed purple). The ITU model does a good job in upper-bounding the AWVR curves for CDs below 70%, but lies

just above the AWVR curves at higher CD values. The light-blue curve (for 2013) contains a partial year's worth of data with much of the data skewed towards the wetter or warmer months. As the 22.2 GHz channel lies very close to the peak of the water vapor absorption line, the spread of the curves  $\sim 5$  K for a given CD below 85% where the ITU curve crosses over the mean AWVR CD curves.

Figure 4b displays the sky brightness CDs of the 23.8 GHz channel for AWVR individual years (solid colors), the AWVR mean (dashed black) and ITU model (dashed purple). The ITU model again does a good job in upper bounding the AWVR curves for CDs below 70%, but lies above most of the AWVR curves at higher CD values. The spread of the CD curves is somewhat smaller, on order of  $\sim 2$  K below the ITU model/AWVR mean cross-over point near 85%. This is consistent with the fact that 23.8 GHz lies further away from the 22.235 GHz water vapor absorption peak.

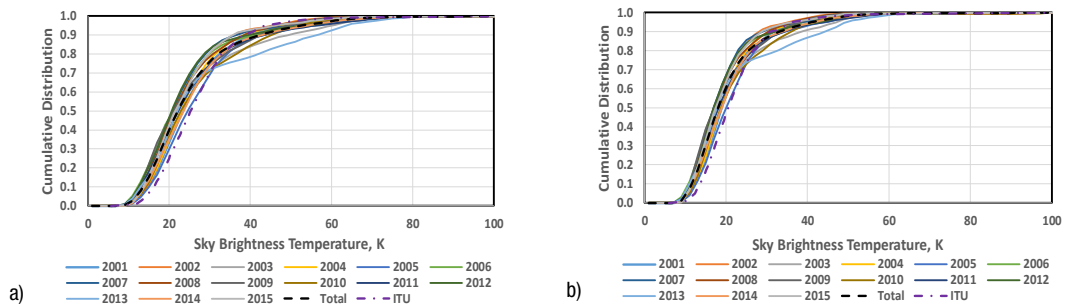


**Figure 4. a) CD of TB at 22.2 GHz: AWVR individual years (solid colors), AWVR mean (dashed black) and ITU model (dashed purple). b) CD of TB at 23.8 GHz: AWVR individual years (solid colors), AWVR mean (dashed black), and ITU model (dashed purple).**

The cumulative distribution of the atmospheric attenuation in the 22.85 GHz band will now be addressed. Since this band is used for uplink only, one only needs to be concerned with atmospheric attenuation and not atmospheric noise temperature. Figure 5a displays the AWVR derived attenuation CD values at 90% (orange points), and the ITU model values (blue) for the three corresponding AWVR frequencies, as well as for frequencies across the 22.85 GHz band. The AWVR and ITU model values at 22.2 GHz and 23.8 GHz are matched to derive scaling coefficients to adjust the ITU points between 22.55 and 23.15 GHz, taking advantage of the water vapor absorption curve shape defined by the ITU model. There is very good agreement between the ITU values and AWVR values at the AWVR frequencies of 22.2 and 23.8 GHz resulting in very little adjustment at the ITU values between 22.55 and 23.15 GHz (red points in plot also tabulated in Table 1). The 31.4 GHz values show more discrepancies and in the reverse direction, as this is likely due to differences in the ITU rain and cloud models, where liquid plays a bigger role at this higher frequency.

Figure 5b displays the atmospheric attenuation at 95% cumulative distribution. The zenith atmospheric attenuation at 95% CD is  $\sim 0.7$  dB. After applying adjustments in a similar manner, the resulting red points in Figure 5b for 22.55 GHz to 23.15 GHz represent the to-be advertised annual attenuation values at 95% CD in this uplink band (also tabulated in Table 2). Here, the adjustments are larger than at 90%, presumably due to the larger

differences in the ITU rain/cloud models. A method using a surface weather model in place of the ITU model to define water vapor absorption curve shape resulted in similar results<sup>2</sup>.

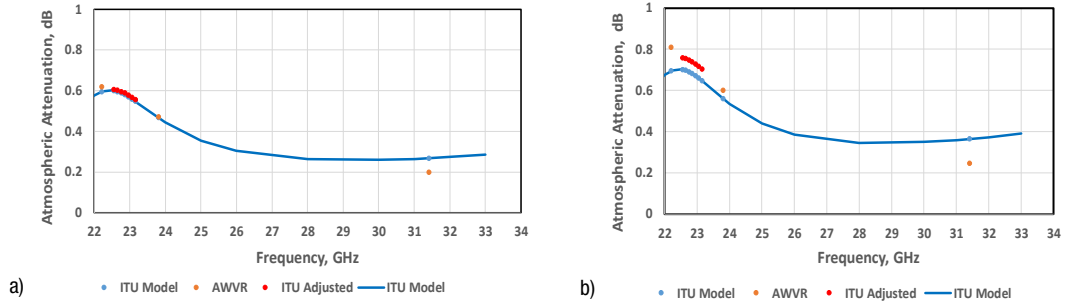


**Figure 5. Goldstone annual atmospheric zenith attenuation vs. frequency, a) 90% CD, b) 95% CD.**

The variation on the Goldstone attenuation statistics was derived in a similar manner, using the best-month (lowest attenuation) and worst-month (highest attenuation) statistics. Here, the cumulative distributions were evaluated for each month over the 15-year span of the AWVR data (2001–2015). For instance, the composite January data consisted of all January data in the 2001–2015 span of AWVR data. The highest and lowest sky brightness temperatures over all 12 months were extracted from the 90% and 95% CD at 22.2 GHz and 23.8 GHz. The resulting attenuation values were then evaluated for use as best-month and worst-month statistics as shown in Table 1 and Table 2. It should be kept in mind that the best-month and worst-month statistics presented here are averages over the 15-year span of data. Thus, there may be single months where the best-month values could be lower and the worst-month values could be higher.

**Table 1. Goldstone Zenith Atmospheric Attenuation  
90% Cumulative Distribution**

Frequency (GHz)	Best Month Attn (dB)	Annual Attn (dB)	Worst Month Attn (dB)
22.55	0.424	0.607	0.893
22.65	0.420	0.603	0.889
22.75	0.413	0.596	0.882
22.85	0.405	0.588	0.874
22.95	0.395	0.578	0.864
23.05	0.384	0.567	0.853
23.15	0.373	0.556	0.842

**Table 2. Goldstone Zenith Atmospheric Attenuation  
95% Cumulative Distribution**

Frequency (GHz)	Best Month Attn (dB)	Annual Attn (dB)	Worst Month Attn (dB)
22.55	0.480	0.759	0.992
22.65	0.476	0.755	0.988
22.75	0.469	0.748	0.981
22.85	0.460	0.739	0.972
22.95	0.449	0.728	0.961
23.05	0.438	0.717	0.950
23.15	0.425	0.704	0.937

Table 1 and Table 2 summarize the annual attenuation values and their best-month and worst-month statistics at 90% and 95% cumulative distribution, respectively, for Goldstone. Note that there is a clear separation in attenuation values as they increase from best month, through annual mean and worst month.

<sup>2</sup> Personal communication, Stephen Slobin, Jet Propulsion Laboratory, Pasadena, California, April 3, 2019.

## B. Madrid, Spain

Ten years of AWVR data spanning the period from 2006 to 2015 were used for the Madrid, Spain analysis. The sky brightness CD curves at 31.4 GHz are shown in Figure 6. Here the individual year curves are shown in solid colors, the mean CD is shown in the black dashed curve, and the CD derived from the ITU model is shown in the dashed purple curve. The difference of the AWVR curves with the ITU curve is likely due to the ITU rain model input used for Madrid.

The AWVR mean CD curve is consistent with that derived from the DSN 810-005 document tables after applying adjustments for cosmic background and frequency difference. These two curves virtually lied on top of each other, providing sufficient confidence in the AWVR data set used here. As seen in Figure 6, the ITU model shows higher values at low CDs. The previous original ITU model showed much higher values at the higher CDs, but the 0.01% rain rate input to the ITU rain model was deemed excessive and a more reasonable rain rate was used [3].

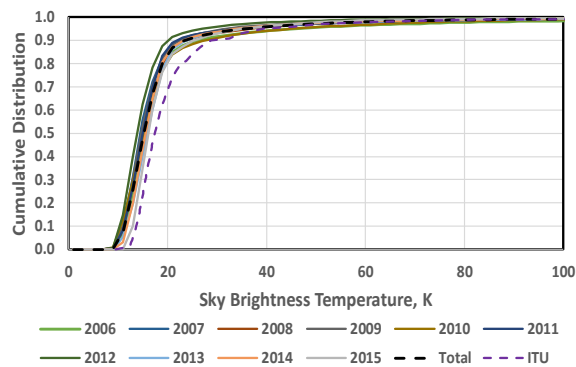


**Figure 6. Cumulative distribution of Madrid AWVR sky brightness temperature at 31.4 GHz for different years (solid colors), annual mean (dashed black), and ITU model (purple).**

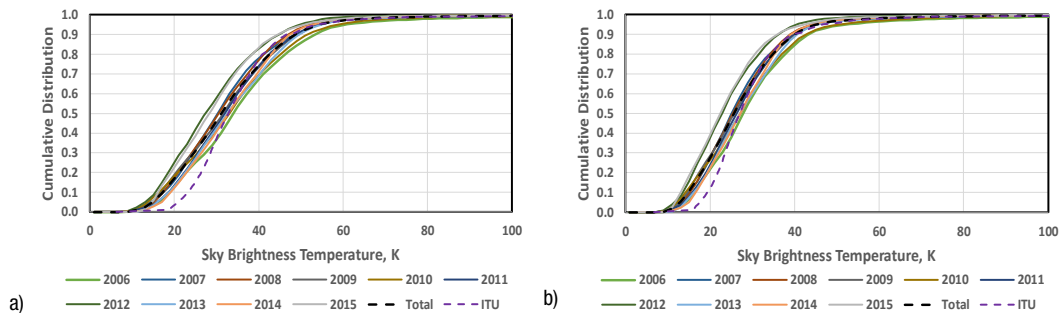


**Figure 7. a) CD of TB at 22.2 GHz, b) CD of TB at 23.8 GHz: AWVR individual years (solid colors), AWVR mean (dashed black) and ITU model (dashed purple).**

The AWVR CD curves for TB at 22.2 and 23.8 GHz were generated along with that of the ITU model at these frequencies for comparison. Figure 7a displays the CD curves for the 22.2 GHz channel for the individual years (solid colors) as well as the AWVR mean over 2006–2015 (dashed black) and ITU model (dashed purple). As 22.2 GHz lies much closer to the frequency of the peak of the water vapor absorption line, the curves differ on order of

as much as ~8 K in TB at low CD values, with the ITU curve crossing higher TB values for a given CD. Since the ITU model provides shape information in the region of the water vapor absorption line, the absolute differences of the ITU model with the AWVR is not important.

Figure 7b displays the CD curves for TB for the 23.8 GHz channel for the individual years from 2006–2015 (solid colors) as well as the AWVR mean (dashed black) and ITU model (dashed purple). The ITU model does a good job in upper bounding the AWVR curves for low CD values. The curves differ again by as much as ~8 K at low CD values. Since this result is similar to that of the 22.2 GHz result in Figure 7a, one can use the AWVR/ITU differences at 22.2 and 23.8 GHz to scale (or adjust) the ITU values between 22.55 and 23.15 GHz to derive the atmospheric attenuation statistics for use in the proposed frequency band.

The atmospheric attenuation at Madrid for 90% cumulative distribution using the ITU model for the proposed uplink frequency band is shown in Figure 8a. The AWVR derived attenuation values are plotted in orange, and the ITU values are plotted in blue for the three AWVR frequencies as well as those across the 22.85 GHz band. The AWVR and ITU values at 22.2 GHz and 23.8 GHz are used to derive scaling coefficients to translate the ITU values between 22.55 and 23.15 GHz, resulting in the red points shown in Figure 8a (also tabulated as annual attenuation values in Table 3). The zenith atmospheric attenuation at 90% CD for this frequency band is ~0.7 dB.

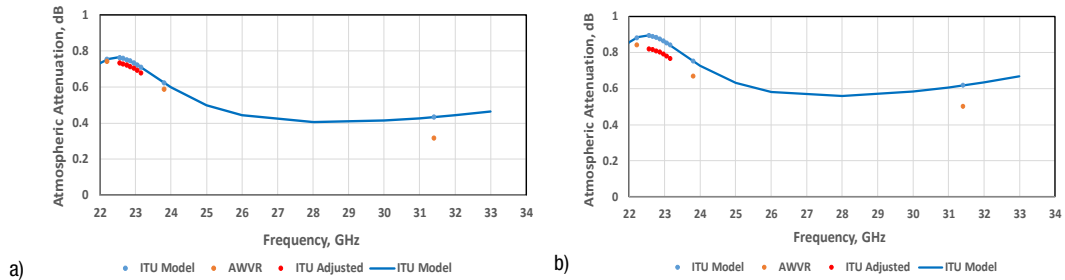


**Figure 8. Madrid zenith attenuation versus frequency a) at 90% CD, b) at 95% CD.**

**Table 3. Madrid Zenith Atmospheric Attenuation 90% Cumulative Distribution**

Frequency (GHz)	Best Month		Worst Month	
	Attn (dB)	Annual Attn (dB)	Attn (dB)	Attn (dB)
22.55	0.615	0.733	0.802	
22.65	0.611	0.729	0.798	
22.75	0.604	0.722	0.791	
22.85	0.596	0.714	0.783	
22.95	0.586	0.704	0.773	
23.05	0.575	0.692	0.762	
23.15	0.564	0.680	0.751	

**Table 4. Madrid Zenith Atmospheric Attenuation 95% Cumulative Distribution**

Frequency (GHz)	Best Month		Worst Month	
	Attn (dB)	Annual Attn (dB)	Attn (dB)	Attn (dB)
22.55	0.760	0.820	0.948	
22.65	0.756	0.816	0.944	
22.75	0.749	0.810	0.937	
22.85	0.740	0.802	0.928	
22.95	0.729	0.791	0.917	
23.05	0.718	0.780	0.906	
23.15	0.705	0.767	0.893	



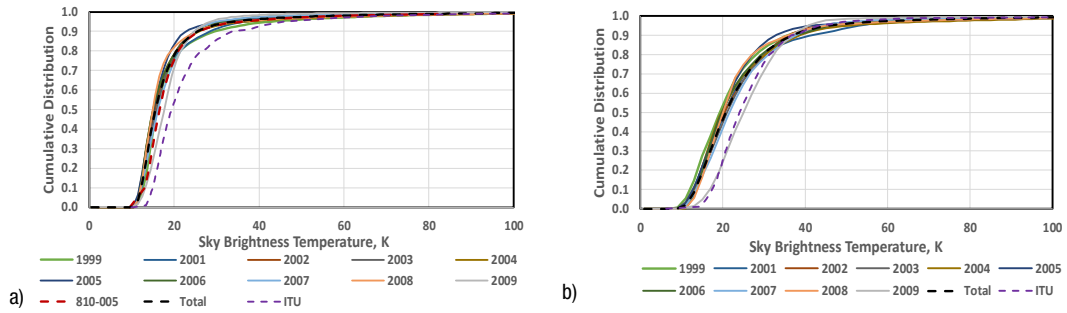
Figure 8b displays the atmospheric attenuation at 95% cumulative distribution for Madrid. The AWVR and ITU values at 22.2 GHz and 23.8 GHz are used to derive scaling coefficients to translate the ITU points between 22.55 and 23.15 GHz, resulting in the red points in Figure 8b (also tabulated as annual attenuation values in Table 4). The zenith atmospheric attenuation at 95% CD is ~0.8 dB. The 31.4 GHz values in Figure 8 shown for informational purposes were not used in the adjustments, as the liquid (rain/cloud model) contribution here is significantly different.

Table 3 and Table 4 summarize the annual mean attenuations for Madrid at 90% and 95%, respectively, as well as the corresponding best-month and worst-month statistics. The best-month and worst-month entries in Table 3 and Table 4 for Madrid have been extracted from the composite months over the 2006–2015 data span in the same manner as was done for Goldstone (Sec. III.A).

### **C. Canberra, Australia**

The WVR used at Canberra, Australia was an older model WVR that was removed from operation in 2010. This WVR only had two channels, one at 20.7 GHz and one at 31.4 GHz (see Figure 1). Given that the Canberra WVR has a frequency channel (20.7 GHz) that lies further away from the water vapor absorption line at 22.235 GHz, a different approach was followed in deriving the 22.55–23.15 GHz band statistics. The WVR data at 20.7 and 31.4 GHz was processed to examine the cumulative distribution of sky brightness temperature at these frequencies. Previously, the 31.4 GHz sky brightness data were reduced to derive the atmospheric attenuation and atmospheric noise temperature statistics quoted in [2]. In addition, since no WVR channels lie inside the proposed band, the curve shape information using the ITU model is required. The TBs from the 20.7 GHz channel of the WVR thus serve as anchor points for appropriately scaling the ITU values. From these results, one could infer the utility of using the ITU model at 22.55 GHz–23.15 GHz. An earlier study documents the comparison between the 810-005 document model (based on WVR measurements) and the ITU model [3].

About ten years of WVR data from Canberra spanning the period from 1999 to 2009 (excluding 2000) was used in this analysis. Figure 9 displays the cumulative distributions for 31.4 GHz and 20.7 GHz. Here, the individual year WVR CDs are shown in solid colors, the mean CD of the WVR data is shown in the black dashed curve, the 31.4 GHz sky temperature CD curve derived from the 810-005 document statistics in dashed red, and the CD derived from the ITU model is shown in the dashed purple curve. The curve for 2009 (light solid purple) is offset to the right from the rest of the annual mean curves as it only contains a partial year of data from January 1 to June 7. Thus, the 2009 curve includes a selection effect favoring the warmer southern hemisphere months and excluding much of the southern hemisphere winter (June–September).



**Figure 9. CD of Canberra WVR TB a) at 31.4 GHz, b) at 20.7 GHz for different years (solid colors), annual mean (dashed black), and ITU model (dashed purple).**

The WVR 31.4 GHz mean sky brightness CD in Figure 9a (dashed black) is consistent with the CD for the TB derived from the 32 GHz atmospheric noise temperature CD in the 810-005 document (after backing out the cosmic background and frequency difference contributions) [2]. The original 810-005 document curves were derived from WVR data covering a different range of time, but the agreement here at 31.4 GHz provides sufficient confidence in the WVR data set. The ITU model is running much higher for any given CD, as previously noted.

The WVR CD curves for TB at 20.7 GHz were generated using the same ITU model at these frequencies for comparison. Figure 9b displays the CD curves for the 20.7 GHz channel TBs for the individual years from 1999 to 2009 (solid colors) as well as the WVR annual mean (“total” dashed black) and ITU model (dashed purple). The individual year CD curves differ by as much as ~5 K below the cross-over point near 85% of the ITU and annual mean WVR curves.

The difference between the 20.7 GHz WVR and 20.7 GHz ITU model values was used to scale the ITU values between 22.55 and 23.15 GHz to generate the attenuation statistics for this band at 90% and 95% CD (see annual statistics in Table 5 and Table 6, respectively).

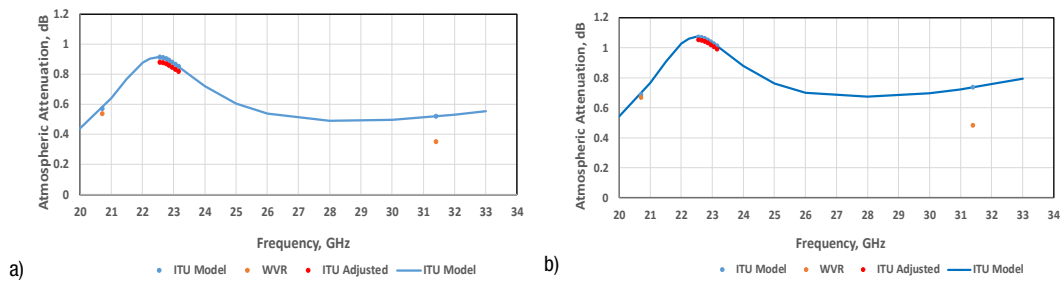


**Figure 10. Atmospheric zenith attenuation versus frequency at Canberra: a) 90%, b) 95%**

**Table 5. Canberra Zenith Atmospheric Attenuation  
90% Cumulative Distribution**

Frequency (GHz)	Best Month Attn (dB)	Annual Attn (dB)	Worst Month Attn (dB)
22.55	0.674	0.878	1.155
22.65	0.670	0.874	1.151
22.75	0.663	0.867	1.144
22.85	0.653	0.857	1.134
22.95	0.641	0.845	1.122
23.05	0.628	0.832	1.109
23.15	0.613	0.817	1.094

**Table 6. Canberra Zenith Atmospheric Attenuation  
95% Cumulative Distribution**

Frequency (GHz)	Best Month Attn (dB)	Annual Attn (dB)	Worst Month Attn (dB)
22.55	0.828	1.053	1.533
22.65	0.824	1.049	1.529
22.75	0.817	1.042	1.522
22.85	0.807	1.032	1.512
22.95	0.796	1.021	1.501
23.05	0.782	1.007	1.487
23.15	0.767	0.992	1.472

The atmospheric attenuation for Canberra at 90% CD using the ITU model is shown in Figure 10a for the proposed 22.55 to 23.15 GHz band, where the WVR derived attenuation values are plotted in orange, and the ITU values are plotted in blue. The ITU values are adjusted to match the WVR values at 20.7 GHz to derive the statistics to be used for frequencies from 22.55 to 23.15 GHz, (shown in red in Figure 10a and given as annual values in Table 5). The zenith atmospheric attenuation at 90% CD is about 0.85 dB.

Figure 10b displays the atmospheric attenuation versus frequency at 95% cumulative distribution. The same method was used to derive 95% attenuation values for the 22.55 to 23.15 GHz band, (shown by the red points in Figure 10b and given as annual values in Table 6). The zenith atmospheric attenuation at 95% CD is about 1 dB.

The best-month and worst-month entries in Table 5 and Table 6 for Canberra have been extracted from the composite months over the 1999–2009 data span in a similar manner as was done for Goldstone (Sec. III.A), and Madrid (Sec. III.B).

Thus, Table 5 and Table 6 summarize the annual mean, best-month and worst-month attenuation statistics for Canberra at 90% and 95% based on the Canberra WVR data reduction analysis at 20.7 GHz. The ITU-model was used to make use of the shape of the water vapor absorption curve in the region covering the 22.55 to 23.15 GHz band.

#### **IV. Conclusion**

A new uplink frequency band (22.55–23.55 GHz) is being investigated for use in lunar communications. As this frequency band lies next to the peak of the water vapor absorption line, atmospheric attenuation statistics were derived from sky brightness temperatures at the lower frequency channels of water vapor radiometers used in the DSN. This article provided details on the approach used to generate these statistics for the three DSN tracking complexes. Atmospheric attenuation annual, best-month and worst-month statistics were presented for atmospheric availabilities of 90% and 95%, which are useful in communication link budget studies.

## Acknowledgements

I would like to thank Kar-Ming Cheung for supporting this work. I would also like to thank Stephen Slobin for providing a detailed review of this paper and for also performing a validation using his surface weather model.

## References

- [1] Report of the Interagency Operations Advisory Group Lunar Communications Architecture Working Group, Issue 1.0, Draft, Co-chairs: Matthew Cosby (UK Space Agency), and Wallace Tai (Jet Propulsion Laboratory, California Institute of Technology).
- [2] S. D. Slobin, "Atmospheric and Environmental Effects," *DSN Telecommunications Link Design Handbook*, DSN No. 810-005, Space Link Interfaces, Module 105, Rev. D, Jet Propulsion Laboratory, Pasadena, California, September 15, 2009. <http://deepspace.jpl.nasa.gov/dsndocs/810-005/105/105D.pdf>
- [3] D. D. Morabito, "A Comparison of Estimates of Atmospheric Effects on Signal Propagation Using ITU Models: Initial Study Results," *The Interplanetary Network Progress Report*, vol. 42-199, Jet Propulsion Laboratory, Pasadena, California, pp. 1-24, November 15, 2014. [https://ipnpr.jpl.nasa.gov/progress\\_report/42-199/199D.pdf](https://ipnpr.jpl.nasa.gov/progress_report/42-199/199D.pdf)
- [4] H. J. Liebe, "Calculated Tropospheric Dispersion and Absorption Due to the 22-GHz Water Vapor Line," *IEEE TRANS on Antennas and Propagation*, vol. AP-17, no. 5, September 1969.
- [5] S. L. Cruz Pol, C. S. Ruf, and S. J. Keihm, "Improved 20- to 32-GHz Atmospheric Absorption Model," *Radio Science*, vol. 33, no. 5, pp. 1319-1333, September-October 1998. <https://agupubs.onlinelibrary.wiley.com/doi/pdf/10.1029/98RS01941>